SCIENTIFIC REPORTS

OPEN

SUBJECT AREAS:
INDUCED PLURIPOTENT STEM CELLS
STEM-CELL BIOTECHNOLOGY
STEM-CELL RESEARCH

Received
29 May 2014

Accepted
19 November 2014

Published
10 December 2014

Correspondence and requests for materials should be addressed to X.W. (xwen@vcu.edu) or N.Z. (nzhang2@vcu.edu)

Formation of Well-defined Embryoid Bodies from Dissociated Human Induced Pluripotent Stem Cells using Microfabricated Cell-repellent Microwell Arrays

Giuseppe Pettinato, Xuejun Wen & Ning Zhang

Institute for Engineering and Medicine, Department of Biomedical Engineering, Chemical and Life Science Engineering, Virginia Commonwealth University, Richmond, VA, 23284 USA.

A simple, scalable, and reproducible technology that allows direct formation of large numbers of homogeneous and synchronized embryoid bodies (EBs) of defined sizes from dissociated human induced pluripotent stem cells (hiPSCs) was developed. Non-cell-adhesive hydrogels were used to create round-bottom microwells to host dissociated hiPSCs. No Rho-associated kinase inhibitor (ROCK-i), or centrifugation was needed and the side effects of ROCK-i can be avoided. The key requirement for the successful EB formation in addition to the non-cell-adhesive round-bottom microwells is the input cell density per microwell. Too few or too many cells loaded into the microwells will compromise the EB formation process. In parallel, we have tested our microwell-based system for homogeneous hEB formation from dissociated human embryonic stem cells (hESCs). Successful production of homogeneous hEBs from dissociated hESCs in the absence of ROCK-i and centrifugation was achieved within an optimal range of input cell density per microwell. Both the hiPSC- and hESC-derived hEBs expressed key proteins characteristic of all the three developmental germ layers, confirming their EB identity. This novel EB production technology may represent a versatile platform for the production of homogeneous EBs from dissociated human pluripotent stem cells (hPSCs).

The emergence of human induced pluripotent stem cells (hiPSCs) represents a milestone in stem cell research. Originally derived from human adult cells by transduction of a combination of four transcription factors, i.e., Oct4, Sox2, C-myc, and Klf4[1], these pluripotent cells exhibit the long-term unlimited self-renewal and pluripotent differentiation capacity similar to human embryonic stem cells (hESCs) while avoiding ethical controversy[2,3]. Similar to hESCs, hiPSCs are capable of differentiating into cells constituting all three somatic germ layers[4]. While hiPSCs hold promises not only as a tool for disease modeling and studying early embryonic development, but also for cell-replacement therapies and drug screening, technical issues remain before their utility can be realized to the full potential. In particular, efficient and directed spontaneous differentiation of hiPSCs into desirable cell lineages with high efficiency in a scalable controlled and reproducible manner is important for therapeutic applications, which require large quantities of one or several specific cell populations. Along the hiPSC differentiation trajectories, embryoid body (EB) formation is a routine inductive step that dictates downstream differentiation for further applications.

EBs are 3-dimentional cell aggregates that mimic some structure of the developing embryo and can differentiate into cells of all three germ layers[5]. EBs are beneficiary in the initiation of lineage-specific differentiation towards many lineages such as cardiac[6,7], neural[8,9], and hematopoietic[10,11]. Although EB permits the generation of cells to all three primary germ layers, the differentiation outcomes are highly dependent upon the quality of EBs, which is affected by the medium conditions[12], the cell numbers, and the sizes of EBs[6,13]. For example, EB viability and the yield in terminal differentiation vary in a size-dependent manner[14]. While too small EBs did not survive well during the differentiation procedures, too large EBs underwent core necrosis[14]. In addition, varying EB sizes

altered the yield in their terminal differentiation towards functional cell lineages[6,13]. There exists an ideal EB size range for best viability and directed differentiation.

Traditional methods in EB formation based upon mechanical dissection of colonies result in colony-derived EBs that are heterogeneous and not reproducible in size and cell population[15]. To ensure that all EBs form from hiPSCs of the same input composition and the formed EBs are spatially and temporally synchronized, dissociated single-cell suspension of hiPSCs is an ideal pathway to take. It also allows tight control of the cell numbers in each EB for size control and consistency. The principle involved in EB production from dissociated single cell suspension deals with the prevention of cell attachment to the culture substrates and promoting cell aggregation while remaining in suspension. To achieve uniform-sized EBs, efforts have been directed towards creating non-adhesive culture surfaces[16] and administering soluble factors in the culture media that promotes cell-cell interactions. Methods such as static suspension culture lack the control over the homogeneity of the environmental factors that individual cells are exposed to, and are not amenable for scalable mass production. In static suspension methods culture, where a suspension of ES cells were seeded to an ultra-low adherence plate or Petri-dish that allows spontaneous aggregation of the cells into spheroids, EBs may randomly fuse together to form large agglomerates which adversely affect cell proliferation and differentiation and may lead to cell death due to the hindrance of mass transport[10]. Static suspension culture produces a wide variety in EB sizes[10]. A more controllable method for EB production involves microwells. Non-adhesive microwells have been used to cultivate dissociated mouse ESCs and promote EB formation[11,17,18]. In this method, dissociated pluripotent stem cells are seeded into small microwells of a volume in the range of several microliters, and allowed/forced to aggregate and grow until they are limited by the size of the microwells. By defining the numbers of ESCs seeded in each separated well and forcing aggregation using centrifuge, this method is able to precisely control EB size and produce homogeneous EBs. However, it requires centrifugation and individual manipulation of the formed EBs manually, and an additional plating step for further culture and maturation. Recently, bioreactors of various designs have been developed to induce EB formation and differentiation in a well-defined scalable manner[19,20]. Bioreactors offer the advantages of easy scale-up EB production, controllable culture parameters, and labor-efficient processing. The scaling-up is highly dependent upon the design of the bioreactors[21]. To control the aggregation of the cells, and therefore, the sizes of the EBs and the mass transport to the cells in culture, stirring/agitation is oftentimes applied. This introduces additional variable of shear stress on the cells. Low-rate stirring results in extensive EB agglomeration that hinder the mass transport, while high-rate stirring is damaging to the cells[22]. Alternatively, rotary vessels are used to provide constant circular motion that improves the efficiency of EB formation[23]. Systems that combine different types of bioreactors[24], encapsulation with bioreactors[25], or static suspension culture followed by bioreactors[24] have been attempted to increase the EB formation and directed differentiation into terminal lineages without compromising the self-renewal stem cell properties of ES cells. Despite these efforts, transplantation of the differentiated cells produced in the bioreactors did not indicate benefits for tissue repair possibly due to micro environmental heterogeneity in the bioreactors that may have altered cell pluripotency and differentiation, giving rise to highly heterogeneous cell populations and disorganized differentiation[26].

It is noteworthy that dissociated hiPSCs are more vulnerable to apoptosis when compared to clusters, resulting in poor EB production from dissociated hiPSCs[27]. Protective agents, such as the Rho-associated kinase (ROCK) inhibitor, Y-27632, was shown to enhance the viability of dissociated single hiPSCs without affecting pluripotency, possibly by preventing anoikis or encouraging cell-cell interactions that lead to aggregation[27]. However, the ROCK inhibitor (ROCK-i) approach involves the administration of a xeno-product that carries the risk of adverse effects or toxicities and may limit the usefulness of the differentiated cells. Little is known about the effects of ROCK-i at the cellular level and what potential cellular damage it could inflict. ROCK-i has been shown to bias cell fate toward residual pluripotency in neural differentiation studies, making these cells unsuitable for cell therapies[28]. A significant drawback of all the existing methods for EB production from dissociated hiPSCs is their reliance on the presence of the ROCK-i. In addition, many of the methods force cell aggregation by centrifugation (i.e., the spin EB method)[11,17,18], which could potentially damage the cells and challenge attempts at automation. In a recent literature review, either ROCK-i or centrifugation has been considered necessary to stimulate dissociated iPSCs to regroup and aggregate during EB formation[29]. Another common disadvantage of the existing methods for EB production is the culture-to-culture variability, which compromises the use of EBs as a model system and a source of differentiated cells for applications in both research and clinical settings. There is an urgent need for a new scalable paradigm to direct well-defined EB formation that allows for subsequent synchronous differentiation into specific cell lineage of interest in a reproducible manner.

In this regard, we have investigated the key parameters in hEB formation and developed a simple scalable technique to allow direct formation of homogeneous and synchronized EBs from dissociated single-cell suspension of hiPSCs without the need of ROCK-i or centrifugation. The environmental conditions applied in each step during the process are well-regulated and standardized for scale-up production and control of cell properties. Naturally occurring agarose, a non-cell-adhesive polysaccharide biomaterial[16,30], was used to create a master mold of microwell configuration to host the dissociated single-cell suspension of hiPSCs. The non-adhesive nature of the agarose microwell led to quick spontaneous aggregation of the hiPSCs to form one EB in each microwell. The size of the EBs was precisely controlled by controlling the initial hiPSC seeding densities in each microwell. The formed EBs can be easily collected manually or robotically. By varying the size of the pillar on the mold, we have been able to fabricate fine agarose microwells via simple stamping. Throughout the process, no ROCK-i, any other xeno-product, nor centrifugation/mechanical disruption was applied. To rule out the reliance of our technique on the presence of the ROCK-i, results from no-ROCK-i and with-ROCK-i conditions were compared. Using our technique, we have been able to produce large numbers of uniform and synchronized EBs of defined sizes. The EBs demonstrated well-organized structures with three distinct germ layers, high viability during prolonged culture, and are capable of multi-lineage differentiation. No core necrosis was observed at any time during the culture. Functional evaluation of the EBs revealed their controlled differentiation into insulin-secreting cells that display the key features of mature pancreatic β-cells pertaining to type 1 diabetes research and therapy. To support the development of our microwell-based system as a platform technology for hEB formation from dissociated human pluripotent stem cells (hPSCs), we have tested side-by-side the system for hEB formation from other hPSC cell lines such as hESC lines. We have tested in the traditional mouse embryonic fibroblasts (MEF) feeder conditions and feeder-free conditions. We have also verified the uniform hEB formation in both mTESR media and E8 media. We have demonstrated the formation of homogeneous hEBs in the absence of ROCK-i and/or centrifugation from dissociated hESCs within a range of input cell density per microwell, in a manner that is similar to the hiPSCs. The resulted hESC EBs were stable in the microwells and underwent growth and stabilization when transferred to suspension culture. The hESC-derived hEBs expressed key proteins characteristic of all three developmental germ layers, confirming their EB identity. The data suggest the compatibility of our agarose microwell-based EB formation approach with

various maintenance culture media systems/conditions of hPSCs. Our method may represent a versatile technological platform that is feasible and practical or controlled reproducible large-scale production of uniform-sized hEBs for research, clinical, and industrial purposes.

Results

Verification of the pluripotency of hiPSCs. Polymerase chain reaction (PCR) revealed that the hiPSCs used in the study expressed the genes known to be associated with undifferentiation state, including OCT4, Sox2[23], Nanog[24], c-Myc, and Klf4, confirming their pluripotency (Supplementary Figure 1). It is important to start with undifferentiated pluripotent stem cells to ensure that their development into EBs is synchronous and to direct their downstream differentiation towards specific cell types.

HiPSCs/hESCs spontaneously formed EBs in the microwells in a cell seeding density-dependent manner. The major finding is that dissociated hiPSCs spontaneously form EBs when plated into the hydrogel microwells in the absence of ROCK inhibitor (ROCK-i) and/or centrifugation (Figure 1); however, the EB formation is highly dependent on the cell seeding numbers. As shown in Figure 1, after 24 hours the hiPSCs spontaneously formed clusters, which were then transferred to suspension culture for further maturation. These clusters had compact appearances after 24 hours in suspension culture, suggesting the development of a normal organized and complex EB structure. EB size distributions were quantified using Image-Pro Plus analysis by measuring the diameter of each EB and calculating the volume since all the EBs were nearly spherical in shape. The formed EBs were highly uniform with an average diameter of 452 ± 48 at the time of extraction and 338 ± 31 at 24 hours after extraction, when 3.5×10^4 cells were seeded. Our examination of the effect of input cell density on EB formation indicated that cell seeding density ranging from 1.5×10^4 to 4.0×10^4 per microwell allowed the formation of uniform-sized EBs with high viability (Figure 2A1 and 2A2). For round-bottom microwells, the best hiPSC cell seeding number was around $3.5 \times 10^4 \pm 1.0 \times 10^3$. In the following experiments, this hiPSC cell seeding density was used for EB formation. We also compared our agarose microwell-based system with the existing commercially available systems such as the V-, and U-bottom plates, and Aggrewell™ plates for hEB formation from the same type of hiPSCs within the same range of input cell density in the absence of centrifugation and ROCK inhibitor. Formation of stable homogenous hEBs from dissociated hiPSCs was not observed in any of the commercially available systems that were tested.

In the absence of ROCK-i and/or centrifugation, we have also achieved homogeneous hEB formation from dissociated single cell suspension of other hPSC lines such as BG01V/hOG hESCs in our microwellls, but within a different range of input cell density per microwell relative to that of hiPSCs (Figure 2B). The range of input cell density per microwell that allowed stable hEB formation from dissociated BG01V/hOG hESCs was 1.0×10^4 to 2.5×10^4. Input cell density beyond this range resulted in disintegration of the aggregates or failure to aggregate by the cells (Figure 2B2). Within this range of input cell density, at 24 hours of incubation, uniform-sized spherical hEBs were formed from dissociated BG01V/hOG hESCs in each microwells (1 hEB per microwell) in the absence of ROCK-i and/or centrifugation under conditions similar to those for dissociated hiPSCs (Figure 2B1). The hEBs exhibited well-defined compact spherical structure with clear rims (Figure 2B2). The formed hEBs were then transferred to suspension culture, where they underwent growth and stabilization.

hEBs exhibited a complex and organized structure. Electron microscopic analysis of the hEBs revealed the presences of a wide variety of junctions, including tight junctions (TJ), gap junctions (GJ), adherens junctions (AJ), and desmosomes (D), confirming a complex and organized structure (Figure 3). Formation of cell-cell junctions inside of the hiPSC EBs (Figure 3A) indicates the readiness of the EBs to differentiate into specialized cells and tissues. In particular, the analysis of hiPSC EBs at different time points (at the time of extraction from the microwells, and after 24 hours and 1 week in suspension culture) showed increased level of internal structural organization as a function of time (Figure 3 A1, A2, A3). In accordance with the results for hiPSC EBs, similar set of junction structures were seen on the hESC EBs at the same set of examination time points after EB formation in the microwells in the absence of ROCK-i and/or centrifugation (Figure 3B). The findings justify our hydrogel microwell-based system in recapitulating at least some aspects of early embryogenesis and differentiation and allowing the generation of not only various cell types in differentiating EBs but also in the tissue-level order similar to what is seen during embryonic development. Next we have examined whether prolonged culture time would allow tissue-level differentiation into more specific tissue types.

Viability of hEBs in a long-term suspension culture. To demonstrate that the hEBs were not transient and sufficiently

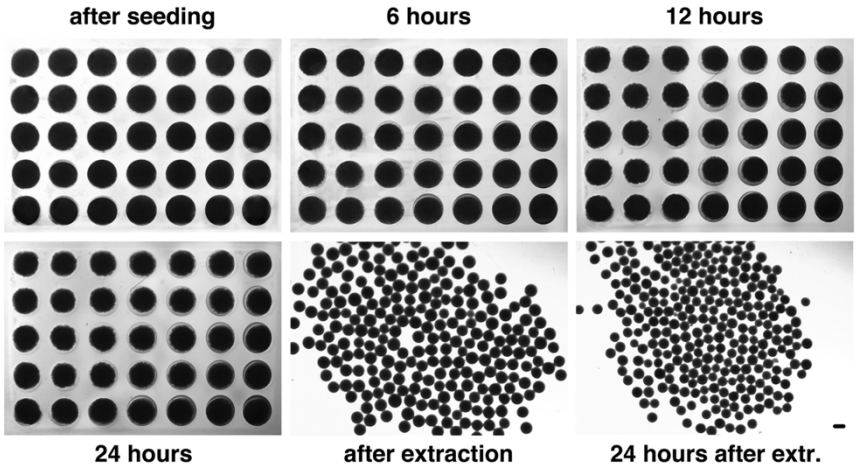

Figure 1 | Time lapse of hEB formation from hiPSCs in the hydrogel microwells at a seeding density of 35,000 hiPSCs/microwell under the no-ROCKi-treatment condition. Condensation of the cell suspension was evident after 6 hr incubation in the hydrogel microwells and continued until hEB extraction after 24 hr incubation. Gross morphology of hEBs that were freshly extracted vs. 24 hrs after extraction.

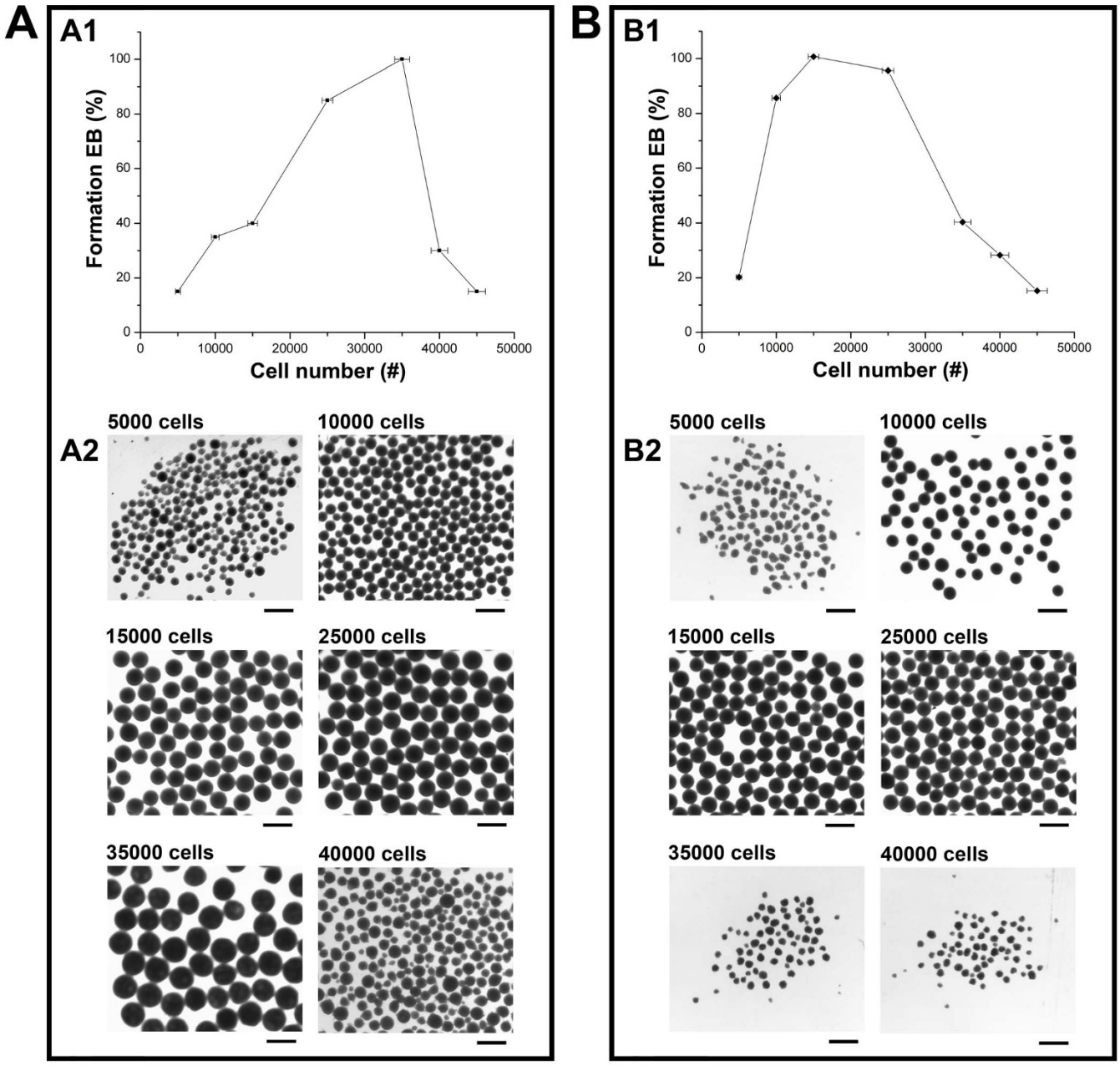

Figure 2 | Examination of the effect of input cell density per microwell on hEB formation from dissociated hiPSCs (A) or BG01V/hOG hESCs (B) under the no-ROCK-i-treatment condition. (A1) The probability of EB formation as a function of input hiPSC cell density per microwell; (A2) Gross morphology of hEBs formed from hiPSCs in the hydrogel microwells at different input cell density per microwell; (B1) The probability of EB formation as a function of input hESC cell density per microwell; (B2) Gross morphology of hEBs formed from hESCs in the hydrogel microwells at different input cell density per microwell. Scale bar = 500 μm.

long-lived to allow further differentiation into specific cell types, we maintained them in suspension culture for 20 days, the period required for the formation of three germ layers during embryogenesis. During the prolonged culture time, the EBs not only maintained high viability and their structures but continued to grow and develop from day 4 following their formation. These findings were independent of the presence of the ROCK-i, as indicated by the lack of difference between the no-ROCK-i and with-ROCK-i conditions throughout the examination period (Figure 4).

Verification for the presence of the three germ layers using gene expression analysis and immunofluorescence. In order to confirm the pluripotency of the produced EBs, it is important to demonstrate that the EBs are able to generate representatives of all three developmental germ layers. As a preliminary assay, we have determined whether the EBs expressed germ layer-specific genes. RT-PCR analysis of the hiPSC EBs which were kept in differentiation medium for 20 days in suspension culture revealed up-regulation of genes associated with each of the three germ layers, including AFP (for endoderm), Sox-1 (for ectoderm), and Brachyury (for mesoderm) (Figure 5A1). Again, no differences between the no-ROCK-i and with-ROCK-i conditions were noted. We also examined the presence of these markers using immunofluorescence localization for the no-ROCK-i condition, and the triple positive staining pattern for the three germ-layer specific markers, i.e., AFP, SOX-1, and BRACHYURY, on the same hiPSC EB clearly confirmed the presence of all three germ layers (Figure 5A2). Same assays were

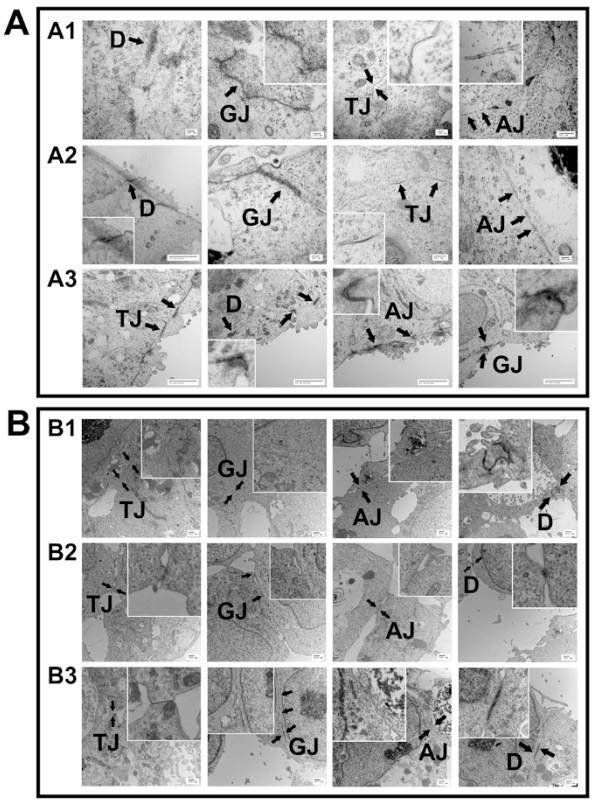

Figure 3 | Transmission electron microscopy examination of the internal structural organization of the hEBs formed from hiPSCs (A) or BG01V/hOG hESCs (B) in the hydrogel microwells under the no-ROCK-i-treatment condition at different time points after extraction (A1, B1) freshly extracted; (A2, B2) 1 day; and (A3, B3) 7 days after extraction. (AJ, adherence junction; GJ, gap junction; D, desmosome; TJ, tight junction).

performed on the hESC EBs, indicating their co-expression of key proteins (i.e., AFP, SOX-1, and BRACHYURY) characteristic of all three developmental germ layers for the no-ROCK-i condition (Figure 5B2). The hESC EBs formed under the with-ROCK-i condition, however, failed to express mesoderm-specific Brachyury at the gene level (Figure 5B1). These data suggest that the loss of pluripotency coincides with differentiation towards the lineages associated with each of the three germ layers and the EB stage represents the onset of hPSC differentiation. These EBs may be amenable to further inductions into specific cell types in high purity given appropriate micro-environmental conditions. In addition to testing hEB formation from dissociated hiPSCs or hESCs that were cultured in mTESR media, as described above, we have achieved homogeneous and synchronized hEB formation in the absence of ROCK-i and/or centrifugation from both dissociated hiPSCs and hESCs that were cultured in feeder-free E8 media and also in traditional MEF-feeder conditions. These results suggest the applicability of our agarose round-bottom microwell-based hEB formation approach to dissociated hPSCs of different lines that are exposed to different culture media systems or conditions during culture process.

hEBs were successfully directed to differentiate into insulin-secreting cells. To demonstrate that hEBs formed with our no-ROCK-i and no-centrifugation approach can be further induced to differentiate into specific tissue lineages, we have sequentially added specific set of soluble factors, including activin A, nicotinamide, and EGF to the cells after EB formation to differentiate them into insulin-producing pancreatic cells. After 21 days of differentiation with our protocol, over 85% of the cells were pancreatic β-cells, as evidenced by the positive staining for Dithizone (DTZ) (Figure 6B DTZ+ in dark crimson red color), a zinc-chelating agent that is known to selectively stain pancreatic β-cells crimson red of their high zinc content[31]. These results suggest that the exposure to certain sets of exogenous factors to the hEBs formed with our no-Rock-i and no-centrifugation approach would override the default endogenous multi-lineage differentiation trajectories with specifications towards more specified lineages, leading to effective production of desired cell types of clinical and research interest. Figure 6A shows the formation of uniform islet-like clusters after 21 days of differentiation. RT-PCR analysis of the differentiated cells revealed the expressions of key pancreatic β-cell-specific genes, e.g., Ngn3, a basic helix-loop-helix transcription factor that is critical for the development of the endocrine cells of the islets, and Pdx-1 (also known as Insulin Promoter Factor 1), a transcriptional factor necessary for pancreatic development and β-cell maturation. The expression of Pdx-1 was also detected at the protein level in Western Blot analysis (Figure 6D), indicating robust up-regulation of PDX-1 under the inductive condition to encourage pancreatic differentiation towards insulin-producing cells. Two key enzymes (endopeptidases or prohormone convertases), i.e., PC-1/3 and PC-2, that regulate the cleavage of specific sites on proinsulin to convert to insulin, were also expressed by the insulin-producing cells. Another enzyme Glucokinase (GK), which plays an important role in the regulation of carbohydrate metabolism as a glucose sensor by facilitating phosphorylation of glucose to glucose-6-phosphate, was weakly expressed by the cells. Other genes that were expressed include, Nkx-6.1, a pancreatic β-cell expressing adenosine triphosphate (ATP)–sensitive potassium (KATP) channels that are necessary for normal insulin secretion, and Sur-1, a protein that modulates KATP channels and insulin release.

Immunocytochemistry staining of insulin indicates that our inductive protocol applied to the hiPSC EBs formed in the agarose microwells has consistently yielded over 80% purity of insulin-secreting cells. Double immunofluorescent staining of insulin and C-peptide revealed their co-localization on the insulin-producing cells (Figure 6E), further confirming a de novo synthesis of insulin which is important to demonstrate the full functionality of our differentiated cells. C-peptide is a by-product when proinsulin is transformed into insulin. Similar to that of pancreatic β-cells in vivo, coupled expression of insulin and GLUT-2, a glucose sensor for insulin-secreting cells, were also documented on the insulin-producing cells that were differentiated from our hiPSC EBs (Figure 6F), suggesting the pancreatic identity of these cells. In the other co-staining group of C-peptide and PDX-1, a master protein for insulin maturation, co-localization of the two markers was observed in some areas of the cell clusters derived from hEBs (Figure 6G), indicative of the formation of mature pancreatic islet-like cells. We have also examined the expression of two pancreatic endocrine hormones glucagon and insulin. At the end of the pancreatic differentiation, glucagon expression was absent from insulin-secreting cells (Figure 6H). The lack of glucagon expression in insulin-positive cells represents the definitive evidence for the terminal differentiation of the hEBs into insulin-producing human pancreatic β-islets and their maturation[32]. No differences between the no-ROCK-i vs. with-ROCK-i conditions were found along any lines of finding.

To further explore the functional characteristics of the hEB-derived cell clusters after pancreatic differentiation, insulin secretion was measured following the end of the differentiation protocol. As shown in Figure 6I, the hEB-derived cell clusters after the pancreatic differentiation exhibited sharp glucose dose dependence in insulin secretion, with significantly lower secretion ($P<0.01$) in response to low glucose concentration (2.8 mM) that mimics basal physiological level relative to that in response to high glucose concentration (25 mM) which represents the high end of the physiological range.

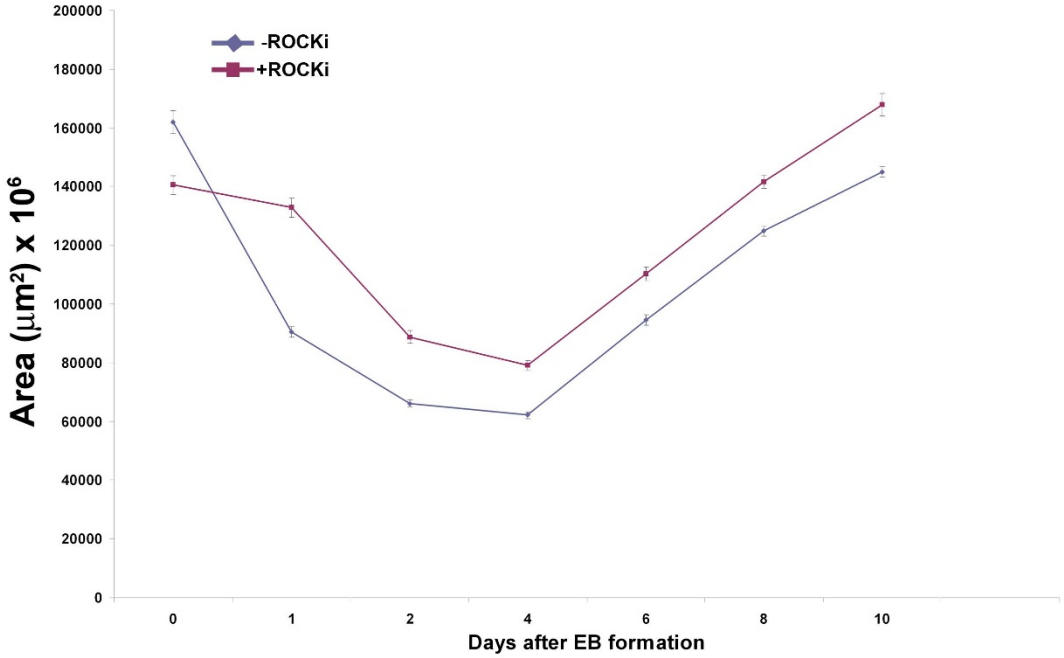

Figure 4 | Time course of the sizes (cross-sectional areas) of hiPSC hEBs after extraction from the hydrogel microwells. –ROCKi: hEBs formed under the no-ROCKi condition; +ROCKi: hEBs formed in the presence of ROCKi. For both conditions, hiPSCs seeding density was 35000 cells per microwell. n = 25.

These data provide fundamental evidence on the glucose-responsive insulin secretion in a physiologic manner, a functional characteristic reminiscent of mature human pancreatic β-cells, for the cell clusters derived from the hEBs produced in our microwell system. In the control group, no insulin secretion was detected in the media collected from the undifferentiated hEBs with both glucose concentrations. Taken together, the insulin-producing cells that were differentiated from our hiPSC EBs displayed the key characteristics typical of mature human pancreatic β-cells.

Discussion

Scalable controlled and reproducible differentiation of human pluripotent stem cells is important to realize their full potential for research, clinical, and industrial purposes, which oftentimes require

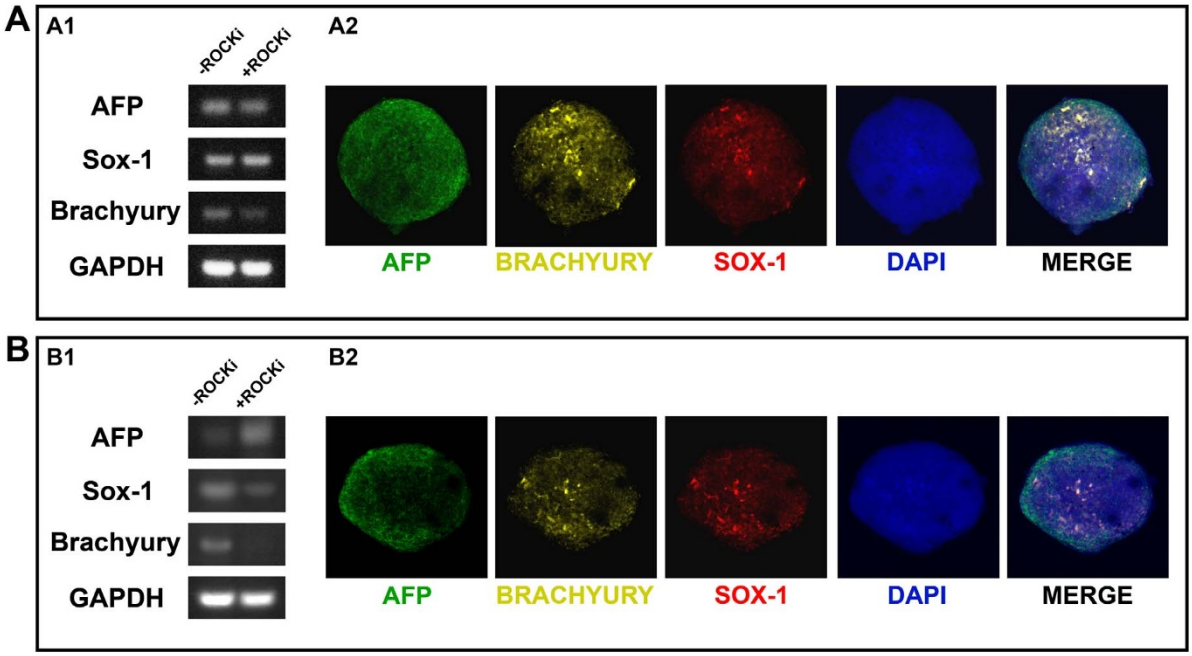

Figure 5 | Expression of molecular markers for the three developmental germ layers by the hiPSC EBs (A) or the BG01V/hOG hESC EBs (B) both at gene and protein levels after 20 days of spontaneous differentiation in suspension culture. –ROCKi: hEBs formed under the no-ROCKi condition; +ROCKi: hEBs formed in the presence of ROCKi. (A1, B1) RT-PCR analysis for gene expression (full-length gel and blot are included in the supplementary information); (A2, B2) Triple immunofluorescence staining showing protein co-expression on a single EB cluster for each cell line under the –ROCKi condition. AFP: alpha feta protein (endoderm-specific), SOX1 (ectoderm-specific), and BRACHYURY (mesoderm-specific). Scale bar = 50 μm.

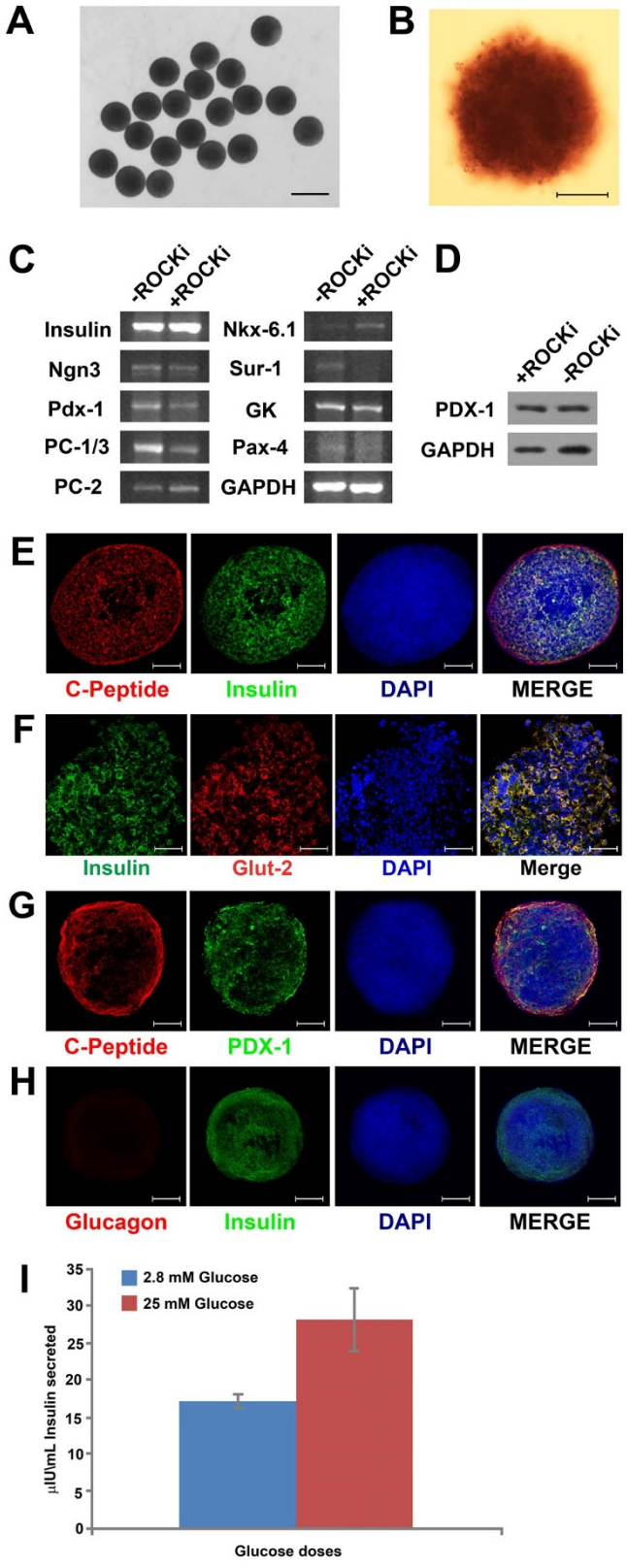

Figure 6 | Differentiation of hiPSC hEBs into insulin-secreting cells. (A) When treated with the pancreatic differentiation protocol for 18 days, hEBs differentiated into islet-like clusters that appeared uniform in sizes and spherical; Scale bar = 1 mm; (B) Over 85% of the cells differentiated from hEBs (formed under no-ROCK-i condition) were pancreatic β-cells, as evidenced by the positive staining for Dithizone (DTZ) in dark crimson red; Scale bar = 200 µm; (C) RT-PCR examination of the expressions of pancreatic lineage-specific genes by the cells after pancreatic differentiation; (D) Western blot analysis of PDX-1, another marker for pancreatic differentiation, in the cells; (E, F, G) Immunostaining of the cells revealed co-localization of insulin (in green) and C-peptide (in red), insulin (in green) and Glut-2 (in red), as well as C-Peptide (in red) and PDX-1 (in green); (H) Co-staining for Glucagon (in red) and Insulin (in green) revealed the absence of glucagon in insulin-secreting cells. Cell nuclei were stained in blue with DAPI. Scale bar = 50 µm; (I) ELISA for insulin secretion assay indicated glucose-responsive insulin secretion from the differentiated cells in a physiologic manner.

large amount of cellular materials of defined lineages. To date, appropriate protocols have not been developed to achieve this goal. EB stage is a routine step in the differentiation protocol of pluripotent stem cells that may dictate downstream differentiation. However, EB is associated with great variability in differentiation due to the inability to standardize its production. Human pluripotent stem cells seem to be more delicate and sensitive to the environment, and therefore, require more stringent conditions for their culture and differentiation[33,34]. Efforts to bypass the EB stage in the differentiation of hiPSCs or standardize EB production have relied on the presence of ROCK inhibitor[35–37]. Our research has focused on overcoming the challenges in the culture and directed differentiation of human pluripotent stem cells. In particular, this study establishes a xeno-free no-ROCK-i no-centrifugation protocol for scalable controlled and reproducible generation of uniform and synchronized EBs from hiPSCs. We have reported for the first time that dissociated hiPSCs cultured on the agarose hydrogel round-bottom microwells began spontaneous aggregation to form one EB per microwell shortly after seeding. Electron microscopic analysis confirmed that these EBs had highly organized structures with extensive formation of cell-cell junctions, including tight junctions, adherence junctions, gap junctions and desmosomes, which have been implicated in the protection of EBs of pluripotent stem cell origin from apoptosis. The EBs had maintained high viability during prolonged culture (the longest time we tested was 30 days), and were capable of robust multi-lineage differentiation as well as directed differentiation into specific lineages. The differentiated cells exhibited all the key characteristics of the desired lineage and could be potentially used for clinical applications and biological studies.

Non-adhesive microwell approach has been adopted for homogeneous EB formation from dissociated hPSCs[38–40]. EBs formed using the microwell approach are oftentimes referred as "spin-EBs" since centrifugation is usually applied in conjunction to force aggregation within the microwells. Existing studies on microwell-based hEB formation from dissociated hPSCs have indicated no success in the absence of centrifugation and/or ROCK-i[11,39,41,42], which may compromise the utility of the hEB-derived cells by potentially biasing cell fate[43], and the scale-up of the process. In our study, non-adhesive round-bottom multiwells were created on agarose hydrogels and we have demonstrated great success in producing large numbers of highly homogeneous and synchronized EBs from dissociated hiPSCs in these round bottom microwells without centrifugation or ROCK-i treatment. Size and shape are important parameters determining the success of EB formation from ESCs or iPSCs and subsequent differentiation[11,44,45]. Control of EB size is not only important to maintain high viability of hiPSCs, but also affect the proliferation and differentiation potential towards specific cell lineages such as cardiomyocytes[6,41], endothelial cells[46], and hematopoietic tissues[11]. For example, germ layer selection of EBs derived from mouse ESCs depended upon the initial size of the EBs: the large EBs (500 µm diameter) showed increased expression of mesodermal and endodermal markers when compared to the smaller EBs (100 µm diameter) which tended to express more ectodermal markers[45]. In the present study, EBs consistently exhibited spherical morphology across all conditions. The size of the EBs, however,

depended upon the initial hiPSC cell seeding density relative to the size of microwells. We speculated that a range of input cell density existed for specific-size microwells that best promoted formation of homogeneous and synchronized EBs. Our examination of the effect of input hiPSC cell density in agarose microwells of a specific size on EB formation confirmed our speculation. The formation of homogenous and synchronized EBs was only allowed with an input hiPSC cell density in the range of 1.5×10^4 to 4.0×10^4 even though the perfect combination between number of cells per EB and viability was observed at the cell density number of 3.5×10^4. Previous studies suggested that the effect of EB size on their differentiation trajectories was mediated through cell-cell interactions[11,44,45] and control within the EBs of the concentration profiles of the soluble factors that are present in the culture medium[14]. While large EBs derived from hESCs encouraged cell-cell interactions that reduced bias towards endodermal differentiation, small EBs favored intercellular communications that increased the expression of endoderm-associated genes[44]. Different-size EBs also varied the accessibilities of the instructive soluble factors that were present in the differentiation medium to cells at different spatial locations within the same EB, therefore, altered the yield in specific differentiation trajectories[14]. The advantage offered by our stamp-press agarose microwells in precisely controlling EB size in a simple, scalable manner may allow tailoring cell-cell interaction that leads to high yields towards specific terminal cell lineages. By optimizing the initial seeding densities in each well, we have achieved average diameter of 452 um on the EBs with a very narrow size distribution.

ROCK inhibitor has been an exclusively inevitable component in all the existing studies on EB formation from dissociated human pluripotent stem cells. Comparison of the no-ROCK-i and with-ROCK-i conditions throughout this study evidences that the ROCK inhibitor was not necessary for the hiPSC culture, EB production, and differentiation using this technology based upon the round-bottom hydrogel microwells. No difference between the no-ROCK-i and with-ROCK-i conditions was found with regard to the viability and pluripotency of EB formed from dissociated hiPSCs. The elimination of ROCK-i is a groundbreaking advantage of this new technique since it obviates the numerous issues associated with ROCK-i, which compromise the usefulness of the differentiated cells in both research and clinical settings. The mechanism involved in the ROCK-i elimination by our system is not clear. However, the properties of the hydrogel microwells, including low-adhesion, controllable size, and geometry, which may contribute to quick cell aggregation and EB formation, therefore reducing the dwelling time of hiPSCs in the state of dissociated single cells for enhanced hiPSC viability[38], may play a role. It is generally accepted in the literatures that from the time of their derivation, hESCs or hiPSCs are best cultured in clusters to prevent dissociation-induced apoptosis and to promote EB formation. The clusters and the cell-cell junctions in these clusters have been shown to be the key to the survival of the cells. Adherens junctions, tight junctions, desmosomes, and gap junctions have all been reported as being cell-cell junctions that help protecting embryonic stem cells from apoptosis[47]. Of particular importance are adherens junctions that are formed by E-cadherin, a key protein that maintains cell-cell contact[48]. Cell-cell junctions of various types were extensively exhibited in our EBs, indicating that our technique encouraged the formation of cell-cell junctions that contribute to cell viability and EB formation.

The demonstration of the robust differentiation of the thus-produced EBs into insulin-producing β–like cells that possess the key characteristics of mature pancreatic β-cells has evidenced the ability of our EB production method to recapitulate the environmental elements during development so that the pluripotency of EBs is preserved. Human pluripotent stem cells represent a promising cell source that is capable of generating transplantable islets for type 1 diabetes mellitus (T1DM) since the conventional whole organ transplantation approach based upon vascularized whole organ allografts or isolated islets is limited due to the critical shortages in cellular/organ donor material, allorejection, and recurrence of autoimmunity. The generation of insulin-producing β–like cells in large quantities in vitro from human pluripotent stem cells provides an abundant cell source that was previously unavailable for research and treatment of type 1 diabetes. Several stepwise protocols exist to differentiate hiPSCs or hESCs into insulin-producing cells in vitro[32,49–51], which are consisted of two steps, i.e., deriving PDX-1 positive pancreatic progenitors from definitive endoderm, and differentiation of PDX-1 positive cells into insulin-producing cells, yet, the culture conditions and the input cell populations in these protocols remain to be optimized to increase the differentiation efficiency. Here we have described a simple protocol using homogeneous and synchronized EBs derived from hiPSCs as the input population for consistency. By simply exposing the EBs to inductive cocktails, we have achieved robust differentiation into insulin-producing β–like cells in high yield. Starting from homogeneous and synchronized EBs has allowed stepwise differentiation that mimics the process of human pancreatic development. Although not the focus of the present study, dissection of the differentiation process has revealed sequential expression of developmental stage-related genes by the EBs with this protocol. At the end of the pancreatic differentiation, the cell clusters derived from hEBs expressed the critical mature human pancreatic β–cell transcription factors and key molecular markers. Examination of pancreatic endocrine hormone expressions indicated the absence of glucagon from insulin-secreting cells, confirming terminally differentiated insulin-producing human pancreatic β-islet identity of the cells[32]. In addition, differentiated cells exhibited sharp glucose dose dependence in insulin secretion in a physiologic manner that was similar to mature human pancreatic β-cells.

This technology for EB formation is considerably fast due to enhanced cell-cell interactions within an ideal range of cell seeding density for a given volume of microwells, facilitating rapid cell aggregation. Enhanced cell-cell interaction is critical in forming cell junctions and activating cell signaling mechanisms that regulate differentiation[52,53]. Several studies have shown enhanced osteogenic differentiation in vitro of mouse ESCs as a result of cell aggregation that occurs in EBs when compared to dissociated single cells[52]. In addition, settled EB cultures demonstrated greater osteogenic differentiation than dissociated EB cultures[52]. These findings concur with a few other studies which reported the benefits of cell-cell interaction and cell-matrix interaction on directed differentiation of stem cells[54,55]. Promotion of cell-cell interaction in mouse EB culture to improve directed pancreatic differentiation was also achieved by introducing additional cell types, such as endothelial cells (ECs), which provide basement membrane components such as laminin and integrins that are critical for insulin gene expression in pancreatic progenitors[53]. Co-culture with ECs was shown to enhance mouse EB differentiation into pancreatic endocrine progenitors and insulin-producing β–like cells primarily in the precise region where EBs and ECs established close cell-cell interaction[53]. In our study, rapid hiPSC cell aggregation in the microwells may have not only boosted cell viability, obviated the need for ROCK inhibitor, but encouraged downstream pancreatic differentiation of the EBs into insulin-producing β–like cells. Our group has also found that it is possible to induce human embryonic stem cells to form EBs without recourse to centrifugation, ROCK-i or any other xenofactors. When plated into hydrogel microwells that discourage cell attachment to the microwell surface, human embryonic stem cells were able to regroup and form EBs within 24 after dissociation. The high-quality of the produced EBs has justified the potential of this method for scale-up and future full automation on the human EB production.

To establish our microwell-based system as a platform technology for homogeneous hEB formation from dissociated hPSCs, we have

tested the system side-by-side for hEB formation from other hPSC cell lines such as BG01V/hOG hESC line. At 24 hours of incubation, uniform-sized spherical hEBs were formed from dissociated hESCs in each microwells (1 hEB per microwell) in the absence of ROCK-i and/or centrifugation under conditions similar to those for dissociated hiPSCs. Examination of the effect of input cell density on EB formation a different range of input hESC density required for stable EB formation from that of hiPSCs. The hESC EBs formed under the no-ROCK-i condition exhibited a complex and increasingly organized structure containing all types of cell-cell junctions with the presences of all three developmental germ layers. The discrepancy in the range of input cell density necessary for stable EB formation from hiPSCs vs. hESCs may be caused by the interline differences among different types of hPSCs. In particular, hiPSCs exhibit a distinct gene expression pattern compared to hESCs[56], which may underlie the difference in their innate differentiation propensity[57]. For both hiPSCs and hESCs, we have also achieved using our microwell-based system in the absence of ROCK-i and/or centrifugation the formation of homogeneous and synchronized hEBs from cells that were maintenance-cultured in different media systems. Taken together, our microwell arrays may offer a versatile platform that is applicable to scale-up production of homogenous hEBs from dissociated hPSCs of a variety of lines that are cultured under various media conditions.

Conclusions

We have demonstrated the proof-of-concept of a hydrogel microwell-based simple technique for homogeneous and synchronized EB formation from dissociated hPSCs. In the absence of ROCK-i and/or centrifugation, thus-produced EBs exhibited well-organized structures with three distinct germ layers, high viability during prolonged culture, and were capable of multi-lineage differentiation as well as directed differentiation into specific lineages. They were amenable to further inductive differentiation into insulin-secreting cells that display the key features of mature pancreatic β-cells. Throughout our process, no ROCK inhibitor, any other xenoproduct, nor centrifugation/mechanical disruption was necessary to achieve cell viability, control EB sizes, or maintain EB structural integrity. Our microwell array-based system may offer a versatile platform for automation and scale-up production of homogeneous hEBs from dissociated hPSCs of different lines that are cultured under various media conditions.

Methods

Human pluripotent stem cell maintenance culture. Feeder-layer-free human induced pluripotent stem (hiPS) cell line derived from foreskin fibroblasts (WiCell Research Institute – WB0002) were expanded in accordance with supplier-recommended protocols. Briefly, hiPSCs were grown on matrigel- coated culture plates (Growth Factor Reduced Matrigel, BD Biosciences) and expanded in chemically defined mTeSR1 medium (mTeSR1 Basal Medium with mTeSR1 5X supplement; Stem Cell Technologies). The colonies were passaged using 0.2 g/L Versene (EDTA) (Lonza) for 8 minutes at room temperature.

BG01V/hOG hESC lines (Invitrogen – R7799-105) were cultured under both traditional MEF feeder conditions and feeder-free conditions using E8 or mTeSR1 Media. In traditional MEF feeder culture condition, BG01V/hOG hESCs were expanded on a feeder layer of mitomycin C-inactivated (10 μg/ml, Invitrogen) MEFs (Millipore) in hESC medium containing DMEM/F12 with 2 mM GLUTAMAX (Invitrogen), 20% (v/v) knockout serum replacement (Invitrogen), 0.1 mM nonessential amino acids (Invitrogen), 55 μM β-mercaptoethanol (Gibco), 4 ng/ml recombinant human bFGF (Inivitrogen), and 50 μg/ml hygromycin B (Invitrogen). StemPro EZPassage tool from Invitrogen was used to separate hESC colonies into uniform pieces. BG01V/hOG hESCs were then transferred to matrigel (Growth Factor Reduced Matrigel, BD Biosciences) and expanded in chemically defined mTeSR1 medium (mTeSR1 Basal Medium with mTeSR1 5X supplement, Stem Cell Technologies). BG01V/hOG hESCs were passaged 5 times to eliminate MEF from the culture.

For the mTeSR1 based culture, the hESCs were culture with the same procedure as described for hiPSCs.

All the hPSCl lines were also cultured in E8 medium (Life Technologies) during maintenance culture in undifferentiated state as xeno-free and feeder-free medium condition. For the human embryoid body formation, parallel experiments were performed using cells cultured under all the culture medium conditions.

Embryoid body formation. Agarose microwell arrays were made using our home-made Teflon stamps. Briefly, the stamps with micropillar array (Supplement Figure 4A) were first designed with SolidWorks (Waltham, MA) and exported into STL file format. The STL file was then transferred to computer numerical controlled (CNC) ultra-high precision lathe (Siemens) to fabricate the micropillars on the Teflon stamp surface. Each micropillar was highly polished. Low-melting-point agarose (Sigma Aldrich) was used to fabricate microwells and form embryoid bodies (EBs) in large quantity from dissociated hiPSCs. The agarose, 20 g/L, was dissolved in 1X phosphate buffered saline (PBS) at 100°C and pipetted into the culture ware. The Teflon stamps were pressed into the agarose solution for approximately 5 min. The agarose gelled in about 2 minutes, the stamps were withdrawn, and microwell array was formed into the gel substrate. The microwell arrays were stored at 37°C in PBS for a prolonged period of time (up to 2 months). No signs of contamination or other stability issues were observed at any time during the storage.

hiPSC colonies were incubated with Accutase (Innovative Cell Technologies) for 5 min at 37°C to form a single-cell suspension. The cell suspensions were centrifuged and counted using an automated cell counting system utilizing dual fluorescence to detect and count the cells, and calculate cell concentration from 20 μl cell sample (Cellometer® Auto 2000 – Nexcelom Bioscience LLC). The counting was performed using a solution containing a combination of the three green-fluorescence nucleic acid stains provided from the same company Nexcelom Bioscience LLC. Using this solution it was possible to obtain an accurate count of the cells, obtaining the different percentages of live and dead cells, that allowed us to plate the desired number of cells into each mold. A 50 μl single-cell suspension was dispensed into each mold in the maintenance medium (Iscove's Modified Dulbecco's Medium [1:1 IMDM, Invitrogen] and F-12 Nutrient Mixture [Ham) (Invitrogen]), 5% fetal bovine serum (Gibco), 1% (vol/vol) insulin transferring selenium-A supplement (Invitrogen), 55 μM monothioglycerol (Sigma Aldrich), 100 U/ml penicillin, and 0.1 mg/ml streptomycin (Gibco).

For EB formation by hiPSCs, 50 μl of cell suspension containing a total of 5,000 to 45,000 cells per well was pipetted into the hydrogel micro-well array. The cell suspension was allowed 10 minutes to settle into the microwells before more maintenance medium was added. To test our method of EB formation against the currently well-known method (exposure to ROCK-i), we compared EB formation with and without exposure to ROCK-i. For the ROCK-i treatment, 10 μM of the ROCK inhibitor was added to the maintenance media. In supplementary figure 3B on the left hand side it is schematized the fabrication of the hydrogel round bottom micro-wells with Teflon stamps. And in the right hand side we show a schematic representation of the hEBs formation process.

Embryonic body suspension culture and growth evaluation. After a 24-hr incubation in the hydrogel microwell array, the hiPSC EBs were aspirated from the wells and placed in suspension culture with the same maintenance medium that was used during EB formation. The iPS EBs were cultured at 37°C and 5% CO2 under gentle agitation using a shaker. The images of the iPS EBs were acquired for diameter measurement using Image Pro Plus (Media Cybernetics, version 4.0). The size was reported as the mean and standard deviation for the batch.

Transmission electron microscopy of cell-cell junctions. The EBs were fixed in 2% glutaraldehyde in 0.1 M cacodylate buffered for 1 hr and rinsed with 0.1 M cacodylate buffered with 0.2 M sucrose. The EB pellets were postfixed in 2% aqueous osmium tetroxide for 1 hr before being rinsed with distilled water. The pellets were dehydrated with a graded ethanol series and embedded in EMbed 812 (Electron Microscopy Sciences, Ft. Washington, PA). Seven-micron-thick sections containing EBs were supported on copper grids and double stained with uranyl acetate in methanol and with Reynolds lead citrate. Cell-cell junctions were imaged using a JEOL 1010 transmission electron microscope.

Embryonic body differentiation. For pancreatic differentiation, 100 ng/ml activin A (PeproTech Inc.), 10 mM nicotinamide (Sigma Aldrich), and 10 ng/ml EGF (Sigma) were added to the culture medium. Differentiation was evaluated after 18 days. The differentiation experiments were performed in triplicate.

DTZ Staining. A DTZ (Merck; Whitehouse Station, NJ; http://www.merck.com) stock solution was prepared with 50 mg of DTZ in 5 ml of dimethyl sulfoxide (DMSO) and stored briefly at −15°C. In vitro DTZ staining was performed by adding 10 μl of the stock solution to 1 ml of culture medium. The staining solution was filtered through a 0.2-μm nylon filter and then used as the DTZ working solution. The culture dishes were incubated at 37°C for 15 minutes in the DTZ solution. After the dishes were thrice rinsed with HBSS, clusters stained crimson red were examined with a stereomicroscope. After examination, the dishes were refilled with DMEM containing 10% FBS. After 5 hours, all traces of stain had disappeared. The number of DTZ-stained cells in the cultures was determined by counting the crimson red cells after trysinization following DTZ stain and averaged over a minimum of 10 microscopic fields for each cluster.

Gene expression analysis. Reverse transcription polymerase chain reaction (RT-PCR) was performed to verify the presence of characteristic gene markers of differentiation. RNA was extracted using Trizol® reagent (Invitrogen) according to the manufacturer's instructions. The RNA concentration and purity was measured using a NanoDrop 2000 spectrophotometer (Thermo-Scientific). The RNA was reverse transcribed to cDNA using the MMLV enzyme (Moloney Murine Leukemia

Virus Reverse Transcriptase, Promega) according to the manufacturer's instructions. One microgram of RNA was used per sample. The cDNA was amplified using Taq polymerase (MBL) according to the manufacturer's instructions. The amplification was performed using the following parameters: one cycle of 94°C for 4 min, 30–35 cycles of denaturation at 94°C for 30 sec followed by annealing at 60°C for 30 sec. The pluripotency of the iPS was confirmed by demonstrating the presence of the undifferentiation genes (ie,Oct4, Sox2, Nanog, cMyc, Klf4. The presence of Alpha Fetoprotein (AFP), Sox1 and Brachyury indicated the presence of three distinct germ layers. Finally, differentiation into fully functional pancreatic cells was identified by confirming the expression of Insulin, Ngn3, Pdx-1, PC-1/3, PC-2, Nkx-6.1, GK and Sur-1. GAPDH was used as a housekeeping gene.

Immunofluorescence visualization of differentiation. For immunolocalization, differentiated EBs were fixed with 4% (wt/vol) paraformaldehyde for 15 min, permeabilized with 0.3% (vol/vol) Triton-X 100 in PBS for 1 hr and blocked with 0.5% (vol/vol) goat serum in PBS for 1 hr. The samples were incubated with the primary antibody at 4°C overnight and then with the secondary antibody at room temperature for 1 hr. The nuclei were stained with 4',6-diamidino-2-phenylindole (DAPI) in PBS for 5 min. The following primary antibodies were used for immunolocalization of insulin (Sigma, I2018, 1 : 100), C-peptide (Abcam, ab30477, 1 : 100), GLUT-2 (Abcam, ab54460, 1 : 100), PDX-1 (Santa Cruz Biotechnology, sc-390808), and Glucagon (Santa Cruz Biotechnology, sc-13091). The secondary antibodies were Cy2-AffiniPure goat anti-mouse IgG, Fc Subclass 1 Specific (Jackson ImmunoResearch, 1 : 100), Cy3-AffiniPure goat anti-rabbit IgG (H+L) (Jackson ImmunoResearch, 1 : 100). The following primary antibodies were used for the three germ layers for the hEBs: mouse anti-alpha 1 fetoprotein (abcam, ab3980, 5 μg/ml), rabbit anti-SOX1 (abcam, ab22572, 4 μg/ml), and goat anti-brachyury (Santa Cruz, as-17743, 1 : 50). The secondary antibodies were Cy2-AffiniPure goat anti-mouse IgG, Fc Subclass 1 Specific (Jackson ImmunoResearch, 1 : 100), Cy3-AffiniPure goat anti-rabbit IgG (H+L) (Jackson ImmunoResearch, 1 : 100), Cy5-conjugated AffiniPure rabbit anti-goat IgG (Jackson ImmunoResearch, 1 : 100). Fluorescent images of the stained EBs after differentiation cultures were acquired with a Leica SP5 confocal microscope and processed by LAS AF Software. The purity of insulin-producing cells was derived by counting the number of insulin-positive cells over the total number of cells in the clusters, and averaged over a minimum of 10 microscopic fields for each cluster.

Western blot analysis. Western blots were performed to detect proteins characteristic of pancreatic differentiation. At the end of the differentiation period, whole proteins were extracted from the cells using RIPA Buffer (25 mM Tris-HCl pH 7.6, 150 mM NaCl, 1% NP-40, 1% sodium deoxycholate, 0.1% SDS, protease inhibitor cocktail (Thermo Scientific)) according to the manufacturer's instructions. The protein content was quantified using the Bradford method (Bio-rad, 500-0006). Absorbance at 595 nm was read using a Spectra max 384 Plus plate reader (Molecular Devices). Protein for each sample, 60 μg, was loaded to perform the electrophoresis in a precast 4-20% SDS-PAGE (Ready Gel Tris-HCl Gel, BioRad) and transferred onto a nitrocellulose membrane (Whatman) with a semi-dry method. The proteins were detected using the following primary antibodies: Rabbit anti-PDX-1 (Abcam, ab47267, 1 : 100) rabbit anti-glyceraldehyde-3-phosphate dehydrogenase (Millipore, MAB374, 1 : 850). Incubations were performed overnight at 4°C. The secondary antibodies used were ECL anti-Rabbit IgG, horseradish peroxidase-linked species-specific whole Ab (GE Healthcare, NA934, 1 : 10000), ECL anti-mouse IgG, horseradish peroxidase-linked species-specific whole Ab (GE Healthcare, NA931, 1 : 10000).

Insulin secretion stimulation and detection. Following the end of the pancreatic differentiation protocol, the cell clusters were washed three times with PBS to eliminate any insulin residues from the differentiation medium. After the washes, the cell clusters were rinsed and incubated in KRBH buffer (118 mM NaCl, 4.7 mM KCl, 1.1 mM KH_2PO_4, 25 mM $NaHCO_3$, 3.4 mM $CaCl_2$, 2.5 mM $MgSO_4$, 10 mM HEPES, and 2 mg/ml BSA) for 1 hr to allow equilibration prior to the stimulation with glucose. The cell clusters were then incubated for 1 hr in KRBH buffer containing 2.8 mM glucose as the basal glucose stimulation buffer before the conditioned buffer was collected. A second incubation of 1 hr was performed in KRBH buffer supplemented with 25 mM glucose (high concentration glucose stimulation). At the end of the incubation, the conditioned buffer was collected and used for the determination of the insulin secretion.

Insulin levels were measured using an enzyme-linked immunosorbent assay (ELISA) Insulin Human Kit (Abcam – ab100578) according to the manufacturer instructions.

1. Takahashi, K. & Yamanaka, S. Induction of pluripotent stem cells from mouse embryonic and adult fibroblast cultures by defined factors. *Cell* **126**, 663–676 (2006).
2. Park, I. H. *et al.* Reprogramming of human somatic cells to pluripotency with defined factors. *Nature* **451**, 141–146 (2008).
3. Wernig, M. *et al.* In vitro reprogramming of fibroblasts into a pluripotent ES-cell-like state. *Nature* **448**, 318–324 (2007).
4. Itskovitz-Eldor, J. *et al.* Differentiation of human embryonic stem cells into embryoid bodies compromising the three embryonic germ layers. *Mol Med* **6**, 88–95 (2000).
5. Hopfl, G., Gassmann, M. & Desbaillets, I. Differentiating embryonic stem cells into embryoid bodies. *Methods Mol Biol* **254**, 79–98 (2004).
6. Mohr, J. C. *et al.* The microwell control of embryoid body size in order to regulate cardiac differentiation of human embryonic stem cells. *Biomaterials* **31**, 1885–1893 (2010).
7. Sargent, C. Y., Berguig, G. Y. & McDevitt, T. C. Cardiomyogenic differentiation of embryoid bodies is promoted by rotary orbital suspension culture. *Tissue Eng Part A* **15**, 331–342 (2009).
8. Kumar, M. *et al.* Neurospheres derived from human embryoid bodies treated with retinoic Acid show an increase in nestin and ngn2 expression that correlates with the proportion of tyrosine hydroxylase-positive cells. *Stem Cells Dev* **16**, 667–681 (2007).
9. Sathananthan, A. H. Neural stem cells in neurospheres, embryoid bodies, and central nervous system of human embryos. *Microsc Microanal* **17**, 520–527 (2011).
10. Dang, S. M., Kyba, M., Perlingeiro, R., Daley, G. Q. & Zandstra, P. W. Efficiency of embryoid body formation and hematopoietic development from embryonic stem cells in different culture systems. *Biotechnol Bioeng* **78**, 442–453 (2002).
11. Ng, E. S., Davis, R. P., Azzola, L., Stanley, E. G. & Elefanty, A. G. Forced aggregation of defined numbers of human embryonic stem cells into embryoid bodies fosters robust, reproducible hematopoietic differentiation. *Blood* **106**, 1601–1603 (2005).
12. Khoo, M. L. *et al.* Growth and differentiation of embryoid bodies derived from human embryonic stem cells: effect of glucose and basic fibroblast growth factor. *Biol Reprod* **73**, 1147–1156 (2005).
13. Messana, J. M., Hwang, N. S., Coburn, J., Elisseeff, J. H. & Zhang, Z. Size of the embryoid body influences chondrogenesis of mouse embryonic stem cells. *J Tissue Eng Regen Med* **2**, 499–506 (2008).
14. Van Winkle, A. P., Gates, I. D. & Kallos, M. S. Mass transfer limitations in embryoid bodies during human embryonic stem cell differentiation. *Cells Tissues Organs* **196**, 34–47 (2012).
15. Joannides, A. J. *et al.* A scaleable and defined system for generating neural stem cells from human embryonic stem cells. *Stem Cells* **25**, 731–737 (2007).
16. Valamehr, B. *et al.* Hydrophobic surfaces for enhanced differentiation of embryonic stem cell-derived embryoid bodies. *Proc Natl Acad Sci U S A* **105**, 14459–14464 (2008).
17. Koike, M., Kurosawa, H. & Amano, Y. A Round-bottom 96-well Polystyrene Plate Coated with 2-methacryloyloxyethyl Phosphorylcholine as an Effective Tool for Embryoid Body Formation. *Cytotechnology* **47**, 3–10 (2005).
18. Koike, M., Sakaki, S., Amano, Y. & Kurosawa, H. Characterization of embryoid bodies of mouse embryonic stem cells formed under various culture conditions and estimation of differentiation status of such bodies. *J Biosci Bioeng* **104**, 294–299 (2007).
19. Lock, L. T. & Tzanakakis, E. S. Expansion and differentiation of human embryonic stem cells to endoderm progeny in a microcarrier stirred-suspension culture. *Tissue Eng Part A* **15**, 2051–2063 (2009).
20. zur Nieden, N. I., Cormier, J. T., Rancourt, D. E. & Kallos, M. S. Embryonic stem cells remain highly pluripotent following long term expansion as aggregates in suspension bioreactors. *J Biotechnol* **129**, 421–432 (2007).
21. Portner, R., Nagel-Heyer, S., Goepfert, C., Adamietz, P. & Meenen, N. M. Bioreactor design for tissue engineering. *J Biosci Bioeng* **100**, 235–245 (2005).
22. Fok, E. Y. & Zandstra, P. W. Shear-controlled single-step mouse embryonic stem cell expansion and embryoid body-based differentiation. *Stem Cells* **23**, 1333–1342 (2005).
23. Gerlach, J. C. *et al.* Dynamic 3D culture promotes spontaneous embryonic stem cell differentiation in vitro. *Tissue Eng Part C Methods* **16**, 115–121 (2010).
24. Yirme, G., Amit, M., Laevsky, I., Osenberg, S. & Itskovitz-Eldor, J. Establishing a dynamic process for the formation, propagation, and differentiation of human embryoid bodies. *Stem Cells Dev* **17**, 1227–1241 (2008).
25. Hwang, Y. S. *et al.* The use of murine embryonic stem cells, alginate encapsulation, and rotary microgravity bioreactor in bone tissue engineering. *Biomaterials* **30**, 499–507 (2009).
26. Taiani, J. T. *et al.* Reduced differentiation efficiency of murine embryonic stem cells in stirred suspension bioreactors. *Stem Cells Dev* **19**, 989–998 (2010).
27. Watanabe, K. *et al.* A ROCK inhibitor permits survival of dissociated human embryonic stem cells. *Nat Biotechnol* **25**, 681–686 (2007).
28. Chaddah, R., Arntfield, M., Runciman, S., Clarke, L. & van der Kooy, D. Clonal neural stem cells from human embryonic stem cell colonies. *J Neurosci* **32**, 7771–7781 (2012).
29. Sheridan, S. D., Surampudi, V. & Rao, R. R. Analysis of embryoid bodies derived from human induced pluripotent stem cells as a means to assess pluripotency. *Stem Cells Int* **2012**, 738910 (2012).
30. Kelm, J. M. *et al.* Design of custom-shaped vascularized tissues using microtissue spheroids as minimal building units. *Tissue Eng* **12**, 2151–2160 (2006).
31. Shiroi, A. *et al.* Identification of insulin-producing cells derived from embryonic stem cells by zinc-chelating dithizone. *Stem Cells* **20**, 284–292 (2002).
32. Kroon, E. *et al.* Pancreatic endoderm derived from human embryonic stem cells generates glucose-responsive insulin-secreting cells in vivo. *Nat Biotechnol* **26**, 443–452 (2008).
33. Takahashi, K. *et al.* Induction of pluripotent stem cells from adult human fibroblasts by defined factors. *Cell* **131**, 861–872 (2007).

34. Yu, J. *et al.* Induced pluripotent stem cell lines derived from human somatic cells. *Science* **318**, 1917–1920 (2007).
35. Chambers, S. M. *et al.* Highly efficient neural conversion of human ES and iPS cells by dual inhibition of SMAD signaling. *Nat Biotechnol* **27**, 275–280 (2009).
36. Nemati, S. *et al.* Long-term self-renewable feeder-free human induced pluripotent stem cell-derived neural progenitors. *Stem Cells Dev* **20**, 503–514 (2011).
37. Kozhich, O. A., Hamilton, R. S. & Mallon, B. S. Standardized Generation and Differentiation of Neural Precursor Cells from Human Pluripotent Stem Cells. *Stem Cell Rev.* Stem Cell Rev **9**, 531–536 (2013).
38. Spelke, D. P., Ortmann, D., Khademhosseini, A., Ferreira, L. & Karp, J. M. Methods for embryoid body formation: the microwell approach. *Methods Mol Biol* **690**, 151–162 (2011).
39. Ungrin, M. D., Joshi, C., Nica, A., Bauwens, C. & Zandstra, P. W. Reproducible, ultra high-throughput formation of multicellular organization from single cell suspension-derived human embryonic stem cell aggregates. *PLoS One* **3**, e1565 (2008).
40. Yukawa, H., Noguchi, H. & Hayashi, S. Embryonic body formation using the tapered soft stencil for cluster culture device. *Biomaterials* **32**, 3729–3738 (2011).
41. Burridge, P. W. *et al.* Improved human embryonic stem cell embryoid body homogeneity and cardiomyocyte differentiation from a novel V-96 plate aggregation system highlights interline variability. *Stem Cells* **25**, 929–938 (2007).
42. Dahlmann, J. The use of agarose microwells for scalable embryoid body formation and cardiac differentiation of human and murine pluripotent stem cells. *Biomaterials* **34**, 2463–2471 (2013).
43. Chaddah, R., Arntfield, M., Runciman, S., Clarke, L. & van der Kooy, D. Clonal neural stem cells from human embryonic stem cell colonies. *J Neurosci* **32**, 7771–7781 (2012).
44. Bauwens, C. L. *et al.* Control of human embryonic stem cell colony and aggregate size heterogeneity influences differentiation trajectories. *Stem Cells* **26**, 2300–2310 (2008).
45. Park, J. *et al.* Microfabrication-based modulation of embryonic stem cell differentiation. *Lab Chip* **7**, 1018–1028 (2007).
46. Hwang, Y. S. *et al.* Microwell-mediated control of embryoid body size regulates embryonic stem cell fate via differential expression of WNT5a and WNT11. *Proc Natl Acad Sci U S A* **106**, 16978–16983 (2009).
47. Smith, A. G. Embryo-derived stem cells: of mice and men. *Annu Rev Cell Dev Biol* **17**, 435–462 (2001).
48. Larue, L., Ohsugi, M., Hirchenhain, J. & Kemler, R. E-cadherin null mutant embryos fail to form a trophectoderm epithelium. *Proc Natl Acad Sci U S A* **91**, 8263–8267 (1994).
49. Jiang, J. *et al.* Generation of insulin-producing islet-like clusters from human embryonic stem cells. *Stem Cells* **25**, 1940–1953 (2007).
50. Tateishi, K. *et al.* Generation of insulin-secreting islet-like clusters from human skin fibroblasts. *J Biol Chem* **283**, 31601–31607 (2008).
51. Zhang, D. *et al.* Highly efficient differentiation of human ES cells and iPS cells into mature pancreatic insulin-producing cells. *Cell Res* **19**, 429–438 (2009).
52. Gothard, D., Roberts, S. J., Shakesheff, K. M. & Buttery, L. D. Engineering embryonic stem-cell aggregation allows an enhanced osteogenic differentiation in vitro. *Tissue Eng Part C Methods* **16**, 583–595 (2010).
53. Talavera-Adame, D. *et al.* Endothelial cells in co-culture enhance embryonic stem cell differentiation to pancreatic progenitors and insulin-producing cells through BMP signaling. *Stem Cell Rev* **7**, 532–543 (2011).
54. Purpura, K. A., Aubin, J. E. & Zandstra, P. W. Sustained in vitro expansion of bone progenitors is cell density dependent. *Stem Cells* **22**, 39–50 (2004).
55. Tian, X. F. *et al.* Comparison of osteogenesis of human embryonic stem cells within 2D and 3D culture systems. *Scand J Clin Lab Invest* **68**, 58–67 (2008).
56. Ghosh, Z. *et al.* Persistent donor cell gene expression among human induced pluripotent stem cells contributes to differences with human embryonic stem cells. *PLoS One* **5**, e8975 (2010).
57. Guenther, M. G. *et al.* Chromatin structure and gene expression programs of human embryonic and induced pluripotent stem cells. *Cell Stem Cell* **7**, 249–257 (2010).

Acknowledgments

This work was made possible by the National Institute for Health of USA (NIH Grant No. NS050243), the Ministry of Science and Technology of China (Grant No. 2012CB966300, 2014CB964600), the National Science Foundation (NSF Grant No. 0748129, 1055922), and William H. Goodwin Endowment Funds.

Author contributions

G.P., X.W. and N.Z. conceived of this study, and participated in its design. G.P. performed the experiments. G.P., X.W. and N.Z. wrote the paper. All authors read and approved the final manuscript.

Additional information

Supplementary information accompanies this paper at http://www.nature.com/scientificreports

Competing financial interests: The authors declare no competing financial interests.

How to cite this article: Pettinato, G., Wen, X. & Zhang, N. Formation of Well-defined Embryoid Bodies from Dissociated Human Induced Pluripotent Stem Cells using Microfabricated Cell-repellent Microwell Arrays. *Sci. Rep.* **4**, 7402; DOI:10.1038/srep07402 (2014).